

Evaluation of experiments on semi-large scale specimens with underclad cracks with focus on constraint and RPV integrity evaluation

Dana Lauerová^{1a}, Vladislav Pištora^{1b}

¹Nuclear Research Institute Řež plc, Řež, Czech Republic

^alau@ujv.cz, ^bpis@ujv.cz

Keywords: cleavage fracture, constraint, reactor pressure vessel, pressurized-thermal shock, FE evaluation, Q-stress parameter, T-stress

Abstract. During years 2005 – 2006, a series of semi-large scale experiments on specimens containing underclad (embedded) crack were performed in NRI Řež. The experiments were performed within EU PHARE project EUROPAID/116529/D/SV/CZ, in cooperation with VTT, FNS, TVONS (Finland) and Tecnomat (Spain). The aim of the project was to investigate fracture mechanics properties of cladding, in particular, to establish the role of cladding in the fracture/failure process of the specimens, and to exploit the obtained knowledge in the procedure for evaluation of integrity of WWER reactor pressure vessels.

Experimental results of the project were described in details e.g. in paper [1]. In the present paper, brief summary of experimental results is provided, and FE evaluation of the experiments is described, with focus on (1) constraint evaluation, and (2) application of the experimental results to the reactor pressure vessel (RPV) integrity evaluation. FE evaluation within point (1) covers, among others, evaluation of J-integral in the moment of cleavage fracture initiation for both upper and lower crack fronts, and evaluation of some type of constraint parameter. Three types of constraint parameter were calculated: T-stress based on elastic calculation, T-stress based on elastic-plastic calculation and Q-stress parameter. In the paper, detailed development of elastic-plastic T-stress as well as Q-stress parameter with loading is presented for one specimen that sustained the highest load. Within point (2), an evaluation of the experiments with respect to the pressurized thermal shocks (PTS) procedure currently being used in the RPV integrity evaluation is performed, and the idea how the results of experiments were used for development of a modified PTS procedure to be used in RPV integrity evaluation in very short future, is briefly described.

Introduction

The main goal of the project EUROPAID/116529/D/SV/CZ was to investigate fracture mechanics behavior of semi-large specimens with underclad (embedded) cracks, and, based on the results obtained, to select proper failure criteria to be used in reactor pressure vessel integrity evaluation. Total number of 11 experiments were performed on specimens with cladding, containing underclad through-thickness crack. The specimens were manufactured from material 15Kh2MFA of Cr-Mo-V type, specially heat treated to simulate the embrittlement of reactor pressure vessel at the end of design life. Several blocks of this material (before heat treatment) were cut from decommissioned not operated reactor pressure vessel of WWER 440 Type NPP Nord. Each of the specimen contained through-thickness crack embedded in the base material, with 3 mm ligament separating the upper crack front from cladding, and was loaded by 4-point-bending at room temperature. During loading, majority of specimens exhibited crack pop-ins followed by ductile tearing of cladding and final failure, only 3 specimens fractured through suddenly, without preceding pop-ins. Evaluation of the experiments within the project concentrated on both process of cleavage fracture in the base material and process of ductile tearing in cladding.

Geometry and loading of the specimens

Test specimens are bars for 4-point bending with nominal dimensions 40 x 85 x 670 mm (BxWxL). Two types of specimens were tested: (1) “normal” specimens (Fig. 1) with nominal crack depth 15 mm and (2) “abnormal” ones (Fig. 2) with nominal crack depth 40 mm and lower crack front blunted to prevent fracture initiation from this crack front. Total number of specimens tested was eleven, eight of them were normal specimens (1E2 – 1E5, 1E9 – 1E12), three were abnormal ones (1E6 – 1E8).

Specimens were subject to 4-point bending, the details of experimental set up are described e.g. in paper [1].

Brief summary of experimental results

During the experiments, total force, LLD and strains in several locations on the upper and flank specimen surfaces were measured. Experimental values of forces at the moment of cleavage initiation (1st pop-in or sudden fracture through) are summarized in Table 1. Majority of specimens exhibited pop-ins during experiments (normal specimens 1E2, 1E3, 1E5, 1E11, 1E12, and all abnormal ones 1E6, 1E7, 1E8), only three specimens fractured through without preceding pop-ins (normal specimens 1E4, 1E9, 1E10). In case of specimens that exhibited pop-ins, the crack propagated towards both bottom and top surfaces of the specimen (in the latter case, into cladding), and arrested.

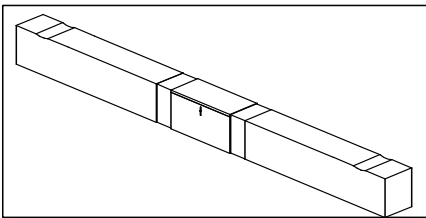


Fig. 1. Scheme of normal specimen.

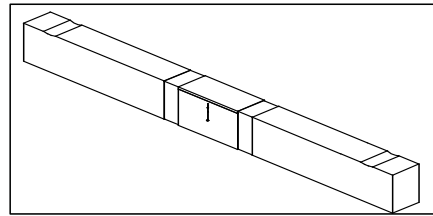


Fig. 2. Scheme of abnormal specimen.

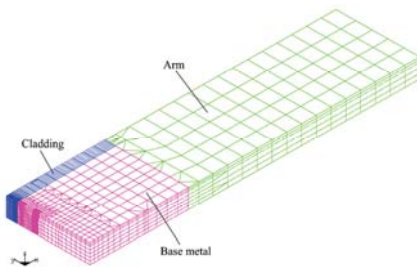


Fig. 3. FE mesh of normal specimen

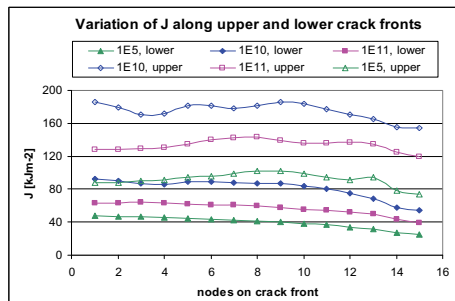


Fig. 4. Variation of J on crack front for 3 specimens

The “depths” of crack propagation into cladding were different for different specimens, and depended, in general, on the energy accumulated in the specimen before the pop-in (the higher was the accumulated energy, the deeper into cladding the crack propagated, but crack arrest, if occurred, always occurred within the first layer of cladding, i.e. within distance of 2 mm from base material (BM) – cladding interface).

FE EVALUATION OF THE EXPERIMENTS

FE post test analyses were performed using FE code SYSTUS. For each of the specimens, a separate 3D FE mesh was constructed, containing approx. 5000 isoparametric quadratic elements. Real crack front shape was modeled, element size near the crack front was 0.2 mm. Due to symmetry of the specimens, only a quarter of the body was modeled (Fig. 3).

For each of the materials modeled (heat treated base metal, heat treated cladding), full stress-strain curves were available and used in the FE calculations. In particular, the following values were used: $R_{p0.2}(BM) = 887.8$ MPa, $R_m(BM) = 984$ MPa, $R_{p0.2}(\text{cladding}) = 338$ MPa, $R_m(\text{cladding}) = 594$ MPa. For modeling plastic properties in FE calculation, flow theory with isotropic hardening and large deformations (updated Lagrangian formulation) were used.

To model residual stresses present in the specimens due to cladding procedure applied to the inner reactor pressure vessel surface, the approach of stress free temperature was used. Stress free temperature of 350 °C was assumed, and corresponding volumetric strains were analytically calculated and then used as input strains (loading) in FE calculation.

For all specimens, the force vs. LLD and force vs. strain curves were calculated and compared with the experimental ones. In majority of cases, a good accordance between experimental and computational curves was reached (see e.g. paper [2]).

For all specimens, values of J-integral along both lower and upper crack fronts at the moment of cleavage initiation (i.e. 1st pop-in or sudden fracture through) were determined, using SYSTUS post-processing module based on theta method (in 3D). The corresponding K_J values at cleavage initiation were determined using plane strain formula $K_J = \sqrt{EJ/(1-\nu^2)}$. Variations of J-integral along both upper and lower (half) crack fronts are, for three selected specimens, seen in Fig. 4. For all specimens, average values of J-integral over upper and lower crack fronts are summarized in Table 1. Besides the J-values, also values of different constraint parameters were calculated, and also Master Curve (MC) approach was utilized.

Based on results of standard specimens, values of MC reference temperature T_0 were determined, for the locations of both crack fronts: $T_0=22.8$ °C for location of upper crack front, and $T_0=19$ °C for location of lower crack front.

Determination of constraint parameters

Various constraint parameters were calculated, such as elastic T-stress, elastic-plastic T-stress, or Q-stress parameter. Values of these constraint parameters were determined for all specimens in the moment of cleavage fracture initiation (1st pop-in or fracture through), the detailed results of comparison of these types of constraint parameters may be found e.g. in paper [2]. In case of specimen 1E4 that sustained the highest load, also the development of both elastic-plastic T-stress and Q-stress parameter with loading was determined and is attached in the present paper.

Determination of T-stress

Values of T-stress were calculated based on either elastic FE calculations (so called “elastic” T-stress, denoted T_{el} in what follows) or elastic-plastic FE calculations (so called “elastic-plastic” T-stress, denoted T_{el-pl} in what follows). They were determined for all specimens in the moment of cleavage fracture initiation (1st pop-in or sudden fracture through). For specimen 1E4, also the development of T_{el-pl} with loading was determined.

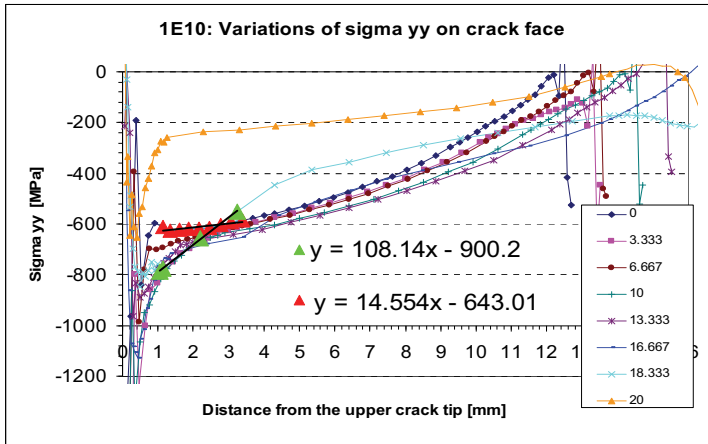


Fig. 5. Elastic-plastic calculation: Variations of σ_{yy} on crack face in different sections along specimen half-thickness (0 – 20 mm), for specimen 1E10.

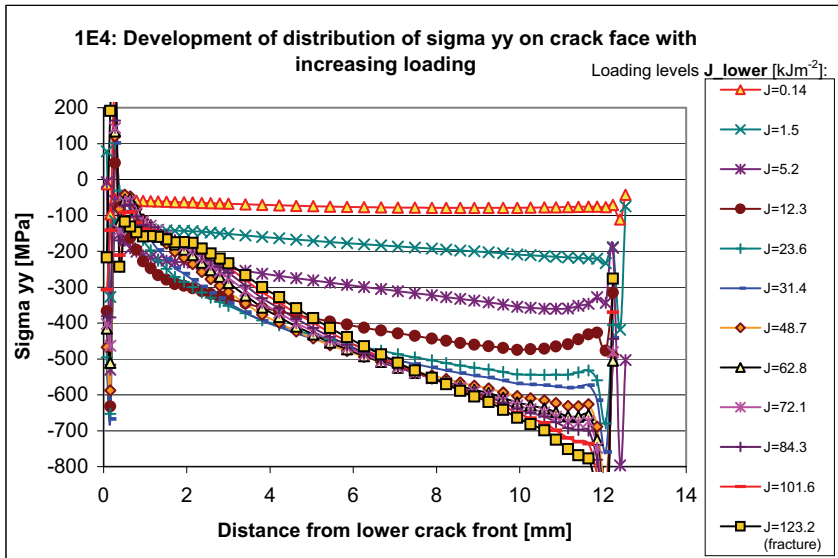


Fig. 6. Elastic-plastic calculation: Development of distribution of σ_{yy} on mid-line of crack face with loading, for 1E4.

Procedure for calculation of T-stress is similar for both cases (T_{el} and T_{el-pl}) and stems from original theoretical definition of T-stress as a second term in Williams expansion series for stress component parallel to the direction of crack propagation: T-stress is obtained as linear extrapolation of “regular” values of σ_{yy} on crack face towards the crack front (“singular” values of σ_{yy} in the vicinity of crack front are not taken into account), where σ_{yy} is component of stress tensor parallel to the direction of crack propagation; for illustration of this procedure see Fig. 5 relevant for determination of T_{el-pl} values at the upper crack front. In this figure, variations of σ_{yy} on crack face in different sections along specimen half-thickness are plotted (for section denoted by “0”, which means longitudinal symmetry plane (LSP), and that one denoted by “18.333”, which means plane

parallel to the LSP, in distance of 18.333 mm from LSP). Performing linear extrapolation of the selected “regular” values of σ_{yy} (large red and green triangles) to the upper crack front ($x=0$), the values of T_{el-pl} appropriate for these two sections (for upper crack front) are obtained, i.e. in this case, -643 MPa and -900 MPa, respectively.

Comparison of T_{el-pl} values with T_{el} ones may be performed based on Table 1, where the appropriate values determined in specimen mid-plane at the moment of cleavage initiation are summarized for both types of T-stress. From this Table it is seen that T_{el-pl} distinguishes between constraint states of the lower and upper crack fronts in a more pronounced way than does the T_{el} : at lower crack front the T_{el-pl} values are higher and at upper crack front smaller than the corresponding T_{el} values (taking into account the sign of T-stress).

In Fig. 6, based on elastic-plastic FE calculation, development of distribution of stress component σ_{yy} on crack face (in the longitudinal symmetry plane of the specimen) with loading is seen, for specimen 1E4 sustaining the highest load. From this figure it is seen that with increasing loading the constraint level (T_{el-pl}) decreases at both crack fronts until the load level of about $J_{lower} \approx 12$ kJm^{-2} , and then at the lower crack front it increases moderately again, while at the upper crack front it continues decreasing until the final fracture.

Determination of Q-stress parameter

Q-stress parameter was determined (based on elastic-plastic FE calculation), for the specimen mid-thickness section only, for each of normal specimens. For calculation of Q the following formula based on crack opening stress (σ_{xx}) was used:

$$Q = \frac{(\sigma_{xx})_{FM} - (\sigma_{xx})_{SSY, T=0}}{\sigma_0} \tag{6}$$

where $(\sigma_{xx})_{FM}$ is stress opening the crack in the “Full Model”, i.e. in the examined specimen; $(\sigma_{xx})_{SSY, T=0}$ is stress opening the crack in reference 2D small scale yielding (SSY) solution with T-stress=0;

$(\sigma_{xx})_{FM}$ was calculated in front of crack front, on line representing the intersection of longitudinal and transversal symmetry planes of the specimen;

σ_0 is the yield stress of the BM ($\sigma_0=887$ MPa). Q-parameter was determined at $r\sigma_0/J=2$.

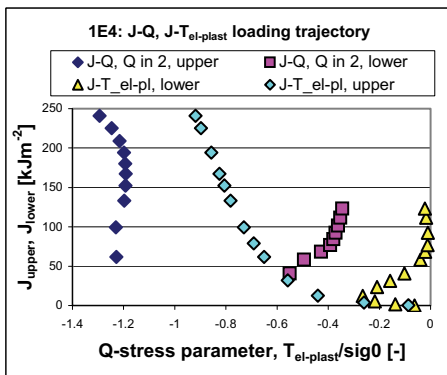


Fig. 7. J-Q, J- T_{el-pl} loading trajectories for 1E4

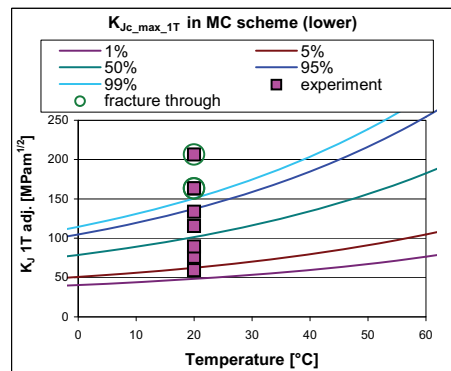


Fig. 8. Experimental data in MC scheme

Q-values determined in the moment of cleavage fracture initiation for individual specimens, together with appropriate J_c -values (i.e. J-Q locus of fracture values), may be found e.g. in [2]; in the presented paper, the attention is focused on development of Q with loading. In Fig. 7, loading

trajectories of J-Q values for specimen 1E4 sustaining the highest load are seen for both lower and upper crack fronts, and, besides of that, they are compared to the appropriate $J-T_{el-pl}/\sigma_0$ loading trajectories. Unfortunately, due to relatively coarse mesh in the vicinity of crack fronts (element size ≈ 0.2 mm), the Q-values could be calculated only starting from certain load level (slightly different for lower and upper crack fronts; for lower crack front this level was about $J_{lower} = 40 \text{ kJm}^{-2}$). In consequence of this, it was not possible to find out whether there is a change in J-Q trajectory trend for lower crack front that would correspond to that one found for $J-T_{el-pl}/\sigma_0$ trajectory for this crack front in Fig. 7 (yellow triangles) and seen qualitatively also in Fig. 6; this change in trend occurs at load level approx. $J_{lower} \approx 12 \text{ kJm}^{-2}$. From Fig. 7 it may be further seen that for higher load levels ($J_{lower} \geq 40 \text{ kJm}^{-2}$), very similar shape of J-Q trajectory for lower crack front to that one of $J-T_{el-pl}/\sigma_0$ trajectory for the same crack front can be seen; for upper crack front, the trajectories shapes differ moderately, but the difference is not substantial (with increasing loading, both constraint factors Q and T_{el-pl}/σ_0 essentially decrease).

Table 1. Values of selected characteristics at the moment of 1st pop-in (or sudden fracture through)

Specimen No.	Force [kN]	Average J for upper crack front [kJm^{-2}]	Average J for lower crack front [kJm^{-2}]	Elastic-plastic T-stress for upper crack front [MPa]	Elastic-plastic T-stress for lower crack front [MPa]	Elastic T for upper crack front [MPa]	Elastic T for lower crack front [MPa]	$Q^*\sigma_0$ for upper crack front [MPa]	$Q^*\sigma_0$ for lower crack front [MPa]
1E2	259.7	53.7	24.3	-581	-114	-433	-227	-1095	-458
1E3	202.8	27.8	12.3	-504	-81	-326	-200	-826	-332
1E4	339.4	240.6	123.2	-848	-15	-626	-352	-1121	-375
1E5	283.2	91.6	39.2	-686	-51	-471	-282	-1127	-499
1E9	315.7	160.4	78.7	-807	-79.1	-539	-297	-1129	-483
1E10	305.9	175	81.6	-621	33	-591	-340	-1009	-340
1E11	278.1	132.6	56.3	-731	-13	-489	-253	-1144	-504
1E12	220.7	47.2	19.2	-519	-101	-376	-217	-1042	-417
1E6	195.8	156	-	-449	-	-298	-	-	-
1E7	205.5	325.3	-	-702	-	-372	-	-	-
1E8	197.3	180.9	-	-577	-	-310	-	-	-

Results of experiments evaluated with respect to RPV integrity assessment

To date, integrity of WWER 440 or WWER 1000 reactor pressure vessels (RPVs) has been assessed using the following procedure: Pressurized thermal shock (PTS) on the inner surface of RPV wall containing postulated semi-elliptical underclad crack with elliptical part of crack front lying in ferritic material (base or weld metal) and straight part in the cladding-ferritic material (FM) interface, is assumed, and it is demonstrated, via FE structural and fracture mechanics calculations, that the crack remains stable during the whole PTS event, i.e. that no initiation of fast fracture occurs from the crack front lying in FM during that time. Within this procedure, K_J -values in all points of crack front lying in FM (that corresponds to the lower crack front in the case of the experiments described) are calculated based on J-values determined from FE calculations, and they are compared to the relevant (with respect to temperature) $[K_{Ic}]_3$ -value, where $[K_{Ic}]_3$ -value means (lower) 5% Master Curve fracture toughness value thickness-adjusted to the crack front length. Essentially, if all K_J -values along crack front lying in FM are smaller than the $[K_{Ic}]_3$ -value, integrity of RPV is proved (details may be found e.g. in [3]). This procedure contains one important assumption: It assumes that integrity of the cladding remains preserved during the PTS event, which means, in other words, that the underclad crack does not become a surface one during the PTS (if this assumption is not fulfilled, a surface crack must be considered, and the appropriate PTS evaluation produces results that are usually much more critical (worse) with respect to the RPV integrity demonstration than in case of underclad crack). However, results of the experiments performed suggest that this assumption is fulfilled:

First, it should be emphasized that within the currently used PTS evaluation procedure the elastic-plastic K_J -values calculated along crack front lying in FM are not constraint corrected. If maximum of these K_J -values is smaller than the $[K_{Ic}]_3$ -value (as explained above), the integrity of reactor pressure vessel is proved for the PTS event considered. But, in addition to this, it should be demonstrated that for these “allowable” K_J -values on the crack front lying in FM, the integrity of cladding is preserved, i.e. that the underclad crack does not become a surface crack during the PTS event. For higher K_J -values than the $[K_{Ic}]_3$ -value, preserving of integrity of cladding is not required, since these values are not admissible from point of view of RPV integrity assessment (of course, in this case, final consequence of not meeting the integrity assessment criteria is adopting certain measures at nuclear power plant to avoid such an adverse situation).

In Fig. 8, cleavage fracture initiation K_{Jc} -values relevant for lower crack front, obtained from the performed experiments for individual semi-large scale specimens, were adjusted to 1 inch thickness (1T) and compared to 1T MC scheme; in this Figure maximum (over lower crack front) K_{Jc} -values are plotted. (This approach is equivalent to that one described above where the calculated K_{Jc} -values do not undergo any adjustment, but the MC scheme is crack front length adjusted.) It is seen from this Figure that 3 specimens that fractured through (they are marked by green open circles) lie high above the level of 5% of the MC probability scheme. Besides of this, majority of other specimens lie also above the 5% MC value, only 1 specimen lies below 5% MC level, but this specimen together with four other specimens underwent crack pop-in only, i.e. their cracks arrested in the cladding, in other words, cladding integrity was preserved during experiments in these cases. Thus, results of experiments suggest, with respect to the current procedure of PTS evaluation, that the following logic is justified and applicable: either the postulated crack is not allowable with respect to fracture initiation in FM (and some measures have to be applied), or assumption of preserving the integrity of cladding during PTS is satisfied

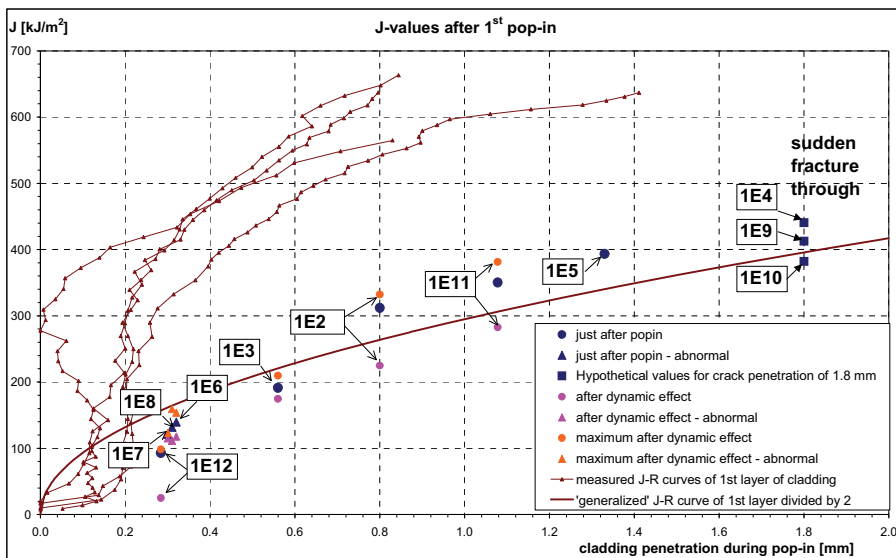


Fig. 9. Comparison of J-values after 1st pop-in to experimental J-R curve for 1st layer of cladding (with large margin). In this manner, the gap in the currently used procedure of RPV integrity evaluation may be considered as covered by the experiments results showing that for PTS during which the applied K_J -values do not exceed 5% MC values, the integrity of cladding is maintained.

In the currently used procedure for PTS evaluation the straight crack front lying in cladding-FM interface is not assessed. However, in very short future, the procedure for PTS evaluation will be

modified in such a manner that the straight crack front should lie 1 mm in the cladding. In association with this, a different approach for assessing the J-values along the straight crack front will be adopted – their values should be compared to the appropriate value of J-R curve for 1st layer of the cladding, with some safety factor. This decision was made based on results of the experiments just described (PHARE Project), in particular, based on the fact that for all experiments that exhibited crack arrest, the crack arrested in the first layer of cladding. The J-values associated with crack arrest in the cladding (i.e. J-values calculated based on FE simulations of pop-ins, via modeling of fast crack propagation with using node release technique) were compared to J-R curve for the 1st layer of cladding; results of this comparison may be seen in Fig. 9. Since a remarkably good agreement between the J-values associated with crack arrest (J-values “just after pop-in” plotted in Fig. 9) and J-R curve values divided by factor 2 was obtained, it was concluded that in the newly proposed procedure for PTS evaluation, the applied J-values calculated for the straight crack front lying 1 mm in cladding should be compared to $J_{1\text{mm}}$ value of J-R curve appropriate for 1st layer of cladding with safety factor of 2, i.e. to $J_{1\text{mm}}/2$.

Summary and conclusion

In the paper, an approximate method for determination of both “elastic” T-stress (T_{el}) and “elastic-plastic” T-stress (T_{el-pl}) was described, stemming from original definition of T-stress as a second term in Williams expansion series for stress component parallel to the direction of crack propagation. This method uses results of FE calculation, in particular, variation of the mentioned stress component on the crack face. Using this method, $J-T_{el-pl}/\sigma_0$ loading trajectories were determined for one specimen sustaining highest load, then they were compared to the corresponding J-Q trajectories (Q determined in $r\sigma_0/J=2$) with the result that both types of trajectories have similar shapes (mainly for lower crack front). This suggests the idea that a consistency in behaviour between the two constraint parameters, elastic-plastic T-stress and Q-stress parameter, may exist.

The experiments performed also suggest that the gap that has existed to date in the PTS evaluation procedure may be considered as covered by the results of experiments showing that the integrity of cladding is preserved during PTS for which the applied K_J -values are “allowable”, i.e. lower than 5% MC fracture toughness values. Based on the experiments performed, a modification of PTS evaluation procedure was proposed. In the modified procedure, the gap mentioned above does not exist – the problem of preserving the cladding integrity is solved numerically: the J-values on straight crack front lying 1mm in cladding are evaluated with using value of $J_{1\text{mm}}/2$ as a criterion, where $J_{1\text{mm}}$ is value of the J-R curve appropriate for 1st layer of cladding, corresponding to crack advance of 1 mm.

References

- [1] Pistora, V., Brumovsky, M., Kohopaa, J., Lauerova, D., Wallin, K.: “Semi-Large Scale Experiments Performed on Specimens with Underclad Cracks”, *19th International Conference on Structural Mechanics in Reactor Technology (SMIRT 19)*, Toronto, Canada, August 12 – 17, 2007.
- [2] Lauerova, D., Pistora, V., Kacor, A., Brumovsky, M.: Evaluation of constraint in semi-large scale experiments performed on specimens with underclad cracks, *19th International Conference on Structural Mechanics in Reactor Technology (SMIRT 19)*, Toronto, Canada, August 12 – 17, 2007.
- [3] Unified Procedure for Lifetime Assessment of Components and Piping in VVER NPPs, VERLIFE, Project of the 5th Framework Programme of the EU, Final version, 2003.